$\sin(\phi_\Lambda - \phi_S)$ azimuthal asymmetry in transversely polarized Λ production in SIDIS within TMD factorization at the EIC

Hui Li,[1] Xiaoyu Wang,[2,*] and Zhun Lu[1,†]

[1]School of Physics, Southeast University, Nanjing 211189, China
[2]School of Physics and Microelectronics, Zhengzhou University, Zhengzhou, Henan 450001, China

(Received 27 April 2021; accepted 22 July 2021; published 18 August 2021)

We investigate the $\sin(\phi_\Lambda - \phi_S)$ single-spin asymmetry in the transversely polarized Λ production in semi-inclusive deeply inelastic scattering process within the transverse momentum dependent (TMD) factorization. The asymmetry is contributed by the convolution of the polarizing TMD fragmentation function $D_{1T}^{\perp}$ of the Λ hyperon and the unpolarized TMD distribution function f_1 of the proton target. We adopt the spectator diquark model result and the available parametrization for $D_{1T}^{\perp,\Lambda^\uparrow/q}$ to numerically estimate the $\sin(\phi_\Lambda - \phi_S)$ asymmetry at the kinematical region of the electron ion collider (EIC). To implement the TMD evolution formalism, we apply two different parametrizations on the nonperturbative Sudakov form factors associated with the distribution function of the proton and the fragmentation function of the Λ. It is found that the two sets of $D_{1T}^{\perp,\Lambda^\uparrow/q}$ lead to different $\sin(\phi_\Lambda - \phi_S)$ asymmetry, particularly in sign. We also discuss the impact of the assumptions and approximations applied in the calculations, which may bring large uncertainties to the results in the EIC. Future measurements on the $\sin(\phi_\Lambda - \phi_S)$ asymmetry with high precision at the EIC can provide important cross checks on the available Λ polarizing fragmentation functions, as well as constrain them more stringently.

DOI: 10.1103/PhysRevD.104.034020

I. INTRODUCTION

Understanding the internal partonic structure of hadrons and the fragmentation mechanism of partons are among the main goals in QCD and high energy physics. Once the production of a polarized lambda hyperon from unpolarized pp collisions had been observed [1,2], it has become a long-standing challenge [3,4] in QCD spin physics since such polarization should be small in leading twist in the collinear picture [3]. The traditional theory expects that the single spin asymmetries should be forbidden in the partonic level, and the averaged polarization of Λ should be zero [4]. Thus, the production of a transversely polarized Λ provides an opportunity not only to study the spin structure [5] but also the fragmentation mechanism [6–10] of partons.

After introducing the intrinsic transverse momentum into the collinear picture, the transverse single spin asymmetry can originate from the correlation of the transverse motion of the parton and the transverse spin of the hadron. It is suggested [11] that a polarizing fragmentation function (FF) [12], denoted by $D_{1T}^{\perp}(x, \boldsymbol{k}_T^2)$, can account for the polarization of the Λ production. $D_{1T}^{\perp}$ is a time-reversal-odd (T-odd) and transverse momentum dependent (TMD) FF, which describes the fragmentation of an unpolarized quark to a transversely polarized hadron, and reflects the correlation of the transverse spin of the produced Λ and the transverse momentum of the parent quark. Sometimes it is viewed as the analog of the Sivers function [13,14], which is a T-odd TMD parton distribution function (PDF) describing the asymmetric density of unpolarized quarks inside a transversely polarized nucleon. Furthermore, $D_{1T}^{\perp}$ may play an important role in the spontaneous polarization, such as the process $q \to \Lambda^\uparrow X$ [15]. Thus, the study on the production of polarized Λ could also provide the information on the spin structure of the hyperon. This is intriguing since the Λ hyperon can not serve as a target in high energy scattering processes.

Experimentally, the single inclusive e^+e^- annihilation (SIA) experiment performed by OPAL at the Large Electron-Positron collider has not observed a significant signal on the transverse polarization of the Λ hyperon [16]. As an alternative to SIA, the processes $e^+e^- \to \Lambda^\uparrow + h + X$ [17–19] and semi-inclusive deep inelastic scattering (SIDIS) $\ell p \to \ell' + \Lambda^\uparrow + X$ have been suggested [17] to study the Λ spin asymmetry, where $D_{1T}^{\perp}$ contribute to the transverse polarization of Λ. Those measurements could

*xiaoyuwang@zzu.edu.cn
†zhunlu@seu.edu.cn

provide a further understanding of the origin of the sizable transverse polarization of hyperons observed in different processes [2,10–12,20–25]. Recently, a nonzero transverse polarization of Λ production in SIA and semi-inclusive $e^+e^- \to \Lambda(\bar{\Lambda}) + K^\pm(\pi^\pm) + X$ processes were measured by the Belle Collaboration [19], making the extraction [26–28] of the polarizing FF of Λ possible. On the other hand, model calculations may also provide an approach to acquire knowledge of the Lambda polarizing FF $D_{1T}^\perp$. A calculation of $D_{1T}^\perp$ for light flavors based on a spectator-diquark model has been performed in Ref. [29], and the result was used to make predictions on physical observables.

The main purpose of this work is to study the role of the polarizing Λ FF $D_{1T}^\perp$ in the transverse-spin dependent $\sin(\phi_\Lambda - \phi_S)$ asymmetry in SIDIS. Particularly, we apply the TMD factorization [30–34] to estimate the spin-dependent cross section in $l + p \to l' + \Lambda^\uparrow + X$, as well as the unpolarized cross section. The asymmetry can be expressed as the ratio of the two cross sections. In the last two decades, TMD factorization has been widely applied in various high energy processes [34–47]. Within the TMD factorization, the differential cross section in the small transverse momentum region $P_{hT}/z_h \ll Q$ (P_{hT} is the transverse momentum of the final-state hadron, and Q is the virtuality of the photon) can be expressed as the convolution of the hard scattering factors and the well-defined TMD distributions and fragmentation functions. In our case, the $\sin(\phi_\Lambda - \phi_S)$ asymmetry is contributed by the convolution of f_1, $D_{1T}^\perp$ and the hard scattering factors. The TMD formalism also encodes the evolution information of TMD PDFs and FFs, governed by the so-called Collins-Soper equation [30,31,34,48]. The solution of the equation is usually expressed as an exponential form of the Sudakov-like form factor [31,34,37,49], which determines the scale dependence of TMDs. Therefore, in this work, we will consider the TMD evolution effect of the polarizing FF $D_{1T}^\perp$, which is not usually included in the previous calculation for the semi-inclusive Λ production [26,27,50]. In the literature, several TMD evolution formalisms have been developed [31,34,37,40,42,44,51–58]. Particularly, the nonperturbative parts of the Sudakov form factor for the TMD PDFs and FFs have been extracted from experimental data based on different parametrizations. In this work, we will adopt two parametrizations on the nonperturbative part to estimate the asymmetry [42,44] for comparison.

The remaining content of the paper is organized as follows. In Sec. II, we present the formalism of the $\sin(\phi_\Lambda - \phi_S)$ asymmetry in the process $lp \to e^-\Lambda^\uparrow X$ within the TMD factorization. In Sec. III, we investigate the evolution effect for the TMD PDFs and FFs. Particularly, we discuss the parametrization of the nonperturbative Sudakov form factors associated with the studied TMD functions in details. In Sec. IV, we present the numerical estimate on the $\sin(\phi_\Lambda - \phi_S)$ asymmetry in the $e^- p \to e^-\Lambda^\uparrow X$ process at the kinematical region of the EIC with different choices on the nonperturbative part associated with the TMD evolution effect. Finally, we summarize the paper in Sec. V.

II. THE $\sin(\phi_\Lambda - \phi_S)$ ASYMMETRY IN THE $lp \to l\Lambda^\uparrow X$ PROCESS

The process under study is the semi-inclusive deep inelastic scattering process,

$$l(\ell) + p(P) \to l(\ell') + \Lambda^\uparrow(P_\Lambda) + X, \tag{1}$$

in which the lepton beam with momentum ℓ scatters off an unpolarized proton target p with momentum P. In the final state, the scattered lepton momentum ℓ' is measured together with a transversely polarized Λ hyperon, with P_Λ being the momentum of the Λ hyperon. We define the spacelike momentum transfer $q = \ell - \ell'$ and $Q^2 = -q^2$. The usual invariants in the SIDIS process are introduced as

$$\begin{aligned} x_B &= \frac{Q^2}{2P\cdot q}, \qquad y = \frac{P\cdot q}{P\cdot \ell} = \frac{Q^2}{x_B s}, \\ z &= \frac{P\cdot P_\Lambda}{P\cdot q}, \qquad s = (P+\ell)^2, \end{aligned} \tag{2}$$

where s is the total center of mass energy squared, x_B is the Bjorken variable, y is the inelasticity, and z is the momentum fraction of the final state Λ hyperon. The corresponding six-fold (x_B, y, z, ϕ_Λ, ϕ_S and $P_{\Lambda T}^2$) differential cross section (for a transversely polarized Λ production) in the $\gamma^* N$ collinear frame can be given as [59–61]

$$\begin{aligned} &\frac{d^6\sigma}{dx_B dy dz d\phi_\Lambda d\phi_S dP_{\Lambda T}^2} \\ &= \frac{\alpha^2}{x_B y Q^2} \times \left\{ \left(1 - y + \frac{1}{2}y^2\right) F_{UUU} \right. \\ &\quad \left. + S_\perp \left[\sin(\phi_\Lambda - \phi_S) \left(1 - y + \frac{1}{2}y^2\right) F_{UUT}^{\sin(\phi_\Lambda - \phi_S)} \right] \right\}. \end{aligned} \tag{3}$$

In the $\gamma^* N$ collinear frame, the momentum direction of the virtual photon is defined as the z-axis, the hadron plane is determined by the z-axis and the momentum direction of Λ, and the lepton plane is given by ℓ and ℓ'. Hence, ϕ_Λ stands for the azimuthal angle between the lepton and hadron planes, while ϕ_S is the azimuthal angle of the transverse spin vector of Λ, $\boldsymbol{P}_{\Lambda T}$ is the component of P_Λ transverse to $\boldsymbol{q}$ with $\boldsymbol{P}_{\Lambda T} = -z q_T$ [62]. Here, $P_{\Lambda T}$ is the characteristic transverse momentum detected in the SIDIS process, the value of which determines the validity of TMD factorization, i.e., if $P_{\Lambda T}^2/z^2 \ll Q^2$, then TMD factorization can be applied, and the process is sensitive to the TMD PDFs/FFs [34]. F_{UUU} and $F_{UUT}^{\sin(\phi_\Lambda - \phi_S)}$ are the spin-averaged and transverse spin-dependent structure functions, with the first, second, and third subscripts denoting the polarization of the lepton beam, proton target, and the final-state hadron (Λ hyperon), respectively (U = unpolarized, L = longitudinally polarized, T = transversely polarized).

We can define the single transverse-spin asymmetry with a $\sin(\phi_\Lambda - \phi_S)$ modulation as follows [60]:

$$A_{UUT}^{\sin(\phi_\Lambda-\phi_S)}(x_B, y, z, P_{\Lambda T}^2) = \frac{\frac{1}{xyQ^2}(1-y+\frac{1}{2}y^2)F_{UUT}^{\sin(\phi_\Lambda-\phi_S)}}{\frac{1}{xyQ^2}(1-y+\frac{1}{2}y^2)F_{UUU}}. \tag{4}$$

According to TMD factorization, the structure functions F_{UUU} and $F_{UUT}^{\sin(\phi_\Lambda-\phi_S)}$ can be expressed as the convolution of the TMD PDF and TMD FF as [60,61]

$$F_{UUU}(Q; P_{\Lambda T}^2) = \mathcal{C}[f_1 D_1], \tag{5}$$

$$F_{UUT}^{\sin(\phi_\Lambda-\phi_S)}(Q; P_{\Lambda T}^2) = \mathcal{C}\left[\frac{\hat{\boldsymbol{h}}\cdot\boldsymbol{k}_T}{M_\Lambda} f_1 D_{1T}^\perp\right], \tag{6}$$

where the unit vector $\hat{\boldsymbol{h}}$ is defined as $\hat{\boldsymbol{h}} = \frac{\boldsymbol{P}_{\Lambda T}}{P_{\Lambda T}}$ [36,63], and the notation $\mathcal{C}$ denotes the convolution of the transverse momenta

$$\mathcal{C}[\omega f D] = x\sum_q e_q^2 \int d^2\boldsymbol{p}_T d^2\boldsymbol{k}_T \delta^2(\boldsymbol{p}_T - \boldsymbol{k}_T + \boldsymbol{q}_T)\omega(\boldsymbol{p}_T, \boldsymbol{k}_T) \times f^q(x, \boldsymbol{p}_T^2) D^q(z, \boldsymbol{k}_T^2), \tag{7}$$

with $\omega(\boldsymbol{p}_T, \boldsymbol{k}_T)$ being an arbitrary function of $\boldsymbol{p}_T$ and $\boldsymbol{k}_T$. Note that $f_1(x_B, \boldsymbol{p}_T^2)$ is the unpolarized TMD PDF of the proton. Also note that $D_1(z, \boldsymbol{k}_T^2)$ and $D_{1T}^\perp(z, \boldsymbol{k}_T^2)$ are the unpolarized FF and the transversely polarizing FF. The transverse momentum $\boldsymbol{k}_T$ is related to the transverse momentum of the produced hadron with respect to the quark through $\boldsymbol{K}_\perp = -z\boldsymbol{k}_T$.

It is convenient to deal with the TMD evolution effect in the $\boldsymbol{b}_\perp$ space that is conjugate to the transverse momentum space through Fourier transformation since it can turn the complicated convolution in the transverse momentum space into simple product. Therefore, we perform a transformation for the delta function

$$\delta^2(\boldsymbol{p}_T - \boldsymbol{k}_T + \boldsymbol{q}_T) = \frac{1}{(2\pi)^2}\int d^2\boldsymbol{b}_\perp e^{-i\boldsymbol{b}_\perp\cdot(\boldsymbol{p}_T - \boldsymbol{k}_T + \boldsymbol{q}_T)} \tag{8}$$

and obtain the following explicit form of the spin-averaged structure function F_{UUU}:

$$\begin{aligned}
\mathcal{C}[f_1 D_1] &= x\sum_q e_q^2 \int d^2\boldsymbol{p}_T d^2\boldsymbol{k}_T \delta^2(\boldsymbol{p}_T - \boldsymbol{k}_T + \boldsymbol{q}_T) f_1^{q/p}(x_B, \boldsymbol{p}_T^2; Q) D_1^{\Lambda/q}(z, \boldsymbol{k}_T^2; Q) \\
&= x\frac{1}{z^2}\sum_q e_q^2 \int d^2\boldsymbol{p}_T d^2\boldsymbol{K}_\perp \delta^2(\boldsymbol{p}_T + \boldsymbol{K}_\perp/z - \boldsymbol{P}_{\Lambda T}/z) f_1^{q/p}(x_B, \boldsymbol{p}_T^2; Q) D_1^{\Lambda/q}(z, \boldsymbol{K}_\perp^2; Q) \\
&= x\frac{1}{z^2}\sum_q e_q^2 \int \frac{d^2\boldsymbol{b}_\perp}{(2\pi)^2} e^{i\boldsymbol{P}_{\Lambda T}\cdot\boldsymbol{b}_\perp/z} \tilde{f}_1^{q/p}(x_B, \boldsymbol{b}_\perp; Q) \tilde{D}_1^{\Lambda/q}(z, \boldsymbol{b}_\perp; Q) \\
&= x\frac{1}{z^2}\sum_q e_q^2 \int \frac{dbb}{2\pi} J_0(P_{\Lambda T} b/z) \tilde{f}_1^{q/p}(x_B, b; Q) \tilde{D}_1^{\Lambda/q}(z, b; Q),
\end{aligned} \tag{9}$$

with $P_{\Lambda T} = |\boldsymbol{P}_{\Lambda T}|$, $b = |\boldsymbol{b}_\perp|$, J_0 the zeroth-order Bessel function of the first kind. The unpolarized PDF and FF in $\boldsymbol{b}_\perp$ space can be defined as (hereafter the tilde terms represent the ones in $\boldsymbol{b}_\perp$ space)

$$\begin{aligned}
\tilde{f}_1^{q/p}(x_B, \boldsymbol{b}_\perp; Q) &= \int d^2\boldsymbol{p}_T e^{-i\boldsymbol{p}_T\cdot\boldsymbol{b}_\perp} f_1^{q/p}(x_B, \boldsymbol{p}_T^2; Q), \\
\tilde{D}_1^{\Lambda/q}(z, \boldsymbol{b}_\perp; Q) &= \int d^2\boldsymbol{K}_\perp e^{-i\boldsymbol{K}_\perp\cdot\boldsymbol{b}_\perp/z} D_1^{\Lambda/q}(z, \boldsymbol{K}_\perp^2; Q).
\end{aligned} \tag{10}$$

Similarly, the transverse spin-dependent structure function $F_{UUT}^{\sin(\phi_\Lambda-\phi_S)}$ can be written as

$$\begin{aligned}\mathcal{C}\left[\frac{\hat{\boldsymbol{h}}\cdot\boldsymbol{k}_T}{M_\Lambda}f_1D_{1T}^{\perp}\right] &= x\sum_q e_q^2\int d^2\boldsymbol{p}_Td^2\boldsymbol{k}_T\delta^2(\boldsymbol{p}_T-\boldsymbol{k}_T+\boldsymbol{q}_T)\frac{\hat{\boldsymbol{h}}\cdot\boldsymbol{k}_T}{M_\Lambda}f_1^{q/p}(x_B,\boldsymbol{p}_T^2;Q)D_{1T}^{\perp\Lambda/q}(z,\boldsymbol{k}_T^2;Q)\\ &= -x\frac{1}{z^3}\sum_q e_q^2\int d^2\boldsymbol{p}_Td^2\boldsymbol{K}_\perp\int\frac{d^2\boldsymbol{b}_\perp}{(2\pi)^2}e^{-i(\boldsymbol{p}_T+\boldsymbol{K}_\perp/z-\boldsymbol{P}_{\Lambda T}/z)\cdot\boldsymbol{b}_\perp}\left(\frac{\hat{\boldsymbol{h}}\cdot\boldsymbol{K}_\perp}{M_\Lambda}\right)f_1^{q/p}(x_B,\boldsymbol{p}_T^2;Q)D_{1T}^{\perp\Lambda/q}(z,\boldsymbol{K}_\perp^2;Q)\\ &= -x\frac{1}{z^3}\sum_q e_q^2\int\frac{d^2\boldsymbol{b}_\perp}{(2\pi)^2}e^{i\boldsymbol{P}_{\Lambda T}\cdot\boldsymbol{b}_\perp/z}\hat{\boldsymbol{h}}_\alpha\tilde{f}_1^{q/p}(x_B,\boldsymbol{b}_\perp;Q)\tilde{D}_{1T}^{\perp(\alpha)\Lambda/q}(z,\boldsymbol{b}_\perp;Q), \end{aligned}\tag{11}$$

where the polarizing FF of Λ hyperon in $\boldsymbol{b}_\perp$ space is defined as

$$\tilde{D}_{1T}^{(\alpha)\perp\Lambda/q}(z,\boldsymbol{b}_\perp;Q) = \int d^2\boldsymbol{K}_\perp e^{-i\boldsymbol{K}_\perp\cdot\boldsymbol{b}_\perp/z}\frac{\boldsymbol{K}_\perp^\alpha}{M_\Lambda}D_{1T}^{\perp\Lambda/q}(z,\boldsymbol{K}_\perp^2;Q). \tag{12}$$

After performing all of the approaches above, the next important issue is the energy dependence of the TMDs, which is encoded in the TMD evolution equations and will be discussed in detail in the following section.

III. THE EVOLUTION OF TMD PDFS AND FFS

In this section, we set up the formalism of the TMD evolution for the unpolarized TMD PDF f_1 of the proton, the unpolarized TMD FF D_1, as well as the polarizing FF $D_{1T}^\perp$ of the Λ hyperon. As mentioned in the previous section, it is more convenient to express the differential cross section of the process in the $\boldsymbol{b}_\perp$ space than in the transverse momentum space. Therefore, the TMD evolution of these TMDs is usually performed in the $\boldsymbol{b}_\perp$ space. Generally, the TMDs $\tilde{F}(x,b;\mu,\zeta_F)$ and $\tilde{D}(z,b;\mu,\zeta_D)$ depend on two energy scales [30,31,34,37,39,55]. One is the renormalization scale μ, related to the corresponding collinear PDFs or FFs; the other one is the energy scale ζ_F (or ζ_D) used as a cutoff to regularize the light-cone singularity in the operator definition of TMD PDFs and FFs. The ζ-dependence is encoded in the Collins-Soper (CS) equation as

$$\frac{\partial\ln\tilde{F}(x,b;\mu,\zeta_F)}{\partial\sqrt{\zeta_F}} = \frac{\partial\ln\tilde{D}(z,b;\mu,\zeta_D)}{\partial\sqrt{\zeta_D}} = \tilde{K}(b;\mu), \tag{13}$$

with $\tilde{K}$ being the CS evolution kernel, which can be computed perturbatively for small values of b with the form (up to order α_s)

$$\tilde{K}(b;\mu) = -\frac{\alpha_sC_F}{\pi}[\ln(\mu^2b^2)-\ln 4+2\gamma_E]+\mathcal{O}(\alpha_s^2). \tag{14}$$

Here, $\gamma_E\approx 0.577$ is the Euler's constant [30]. The μ dependence is driven by the renormalization group equations as

$$\frac{d\tilde{K}}{d\ln\mu} = -\gamma_K(\alpha_s(\mu)), \tag{15}$$

$$\frac{d\ln\tilde{F}(x,b;\mu,\zeta_F)}{d\ln\mu} = \gamma_F\left(\alpha_s(\mu);\frac{\zeta_F^2}{\mu^2}\right), \tag{16}$$

$$\frac{d\ln\tilde{D}(z,b;\mu,\zeta_D)}{d\ln\mu} = \gamma_D\left(\alpha_s(\mu);\frac{\zeta_D^2}{\mu^2}\right), \tag{17}$$

where γ_K, γ_F, and γ_D are the anomalous dimensions of $\tilde{K}$, $\tilde{F}$, and $\tilde{D}$, respectively,

$$\gamma_K = 2\frac{\alpha_sC_F}{\pi}+\mathcal{O}(\alpha_s^2), \tag{18}$$

$$\gamma_D = \gamma_F = \alpha_s\frac{C_F}{\pi}\left(\frac{3}{2}-\ln\left(\frac{\zeta_F}{\mu^2}\right)\right)+\mathcal{O}(\alpha_s^2). \tag{19}$$

Solving the equations in Eqs. (15)-refeq:evol3), one can obtain the general solution for the energy dependence of $\tilde{F}$ and $\tilde{D}$ as follows:

$$\tilde{F}(x,b;Q) = \mathcal{F}(Q)\times e^{-S(Q,b)}\times\tilde{F}(x,b;\mu_i), \tag{20}$$

$$\tilde{D}(z,b;Q) = \mathcal{D}(Q)\times e^{-S(Q,b)}\times\tilde{D}(z,b;\mu_i), \tag{21}$$

where $\mathcal{F}$ and $\mathcal{D}$ are the hard factors related to the hard scattering, and $S(Q,b)$ is the Sudakov form factor. Hereafter, we will set $\mu=\sqrt{\zeta_F}=\sqrt{\zeta_D}=Q$ and express $\tilde{F}(x,b;\mu=Q,\zeta_F=Q^2)$ and $\tilde{D}(z,b;\mu=Q,\zeta_D=Q^2)$ for simplicity. Equations (20) and (21) demonstrate that the TMDs $\tilde{F}$ and $\tilde{D}$ at the arbitrary scale Q can be determined by the same TMDs at an initial scale μ_i through the evolution encoded by the exponential form, $\exp(-S(Q,b))$ [30–34,48,64].

More specifically, the exponential $\exp(-S(Q,b))$ has the following explicit form (taking the one for $\tilde{F}$ as example):

$$\begin{aligned}
&\exp(-S(Q,b)) \\
&\quad = \exp\left\{\ln\frac{Q}{\mu}\tilde{K}(b_*;\mu)\right. \\
&\qquad \left. + \int_{\mu_i}^{\mu}\frac{d\bar{\mu}}{\bar{\mu}}\left[\gamma_F(g(\bar{\mu});1) - \ln\left(\frac{Q}{\bar{\mu}}\right)\gamma_K(g(\bar{\mu}))\right]\right\} \\
&\qquad \times \exp\left\{g_{j/P}(x,b) + g_K(b)\ln\frac{Q}{Q_0}\right\}.
\end{aligned} \tag{22}$$

The exponential in the first line of Eq. (22) comes from the solutions of Eqs. (13), (15), and (16) in the perturbative region (the small b region $1/Q \ll b \ll 1/\Lambda$). It contains $\tilde{K}(b_*;\mu)$, the CS evolution kernel in the small b region, and the anomalous dimension γ_F, γ_K. However, in the nonperturbative region (large b region), the evolution kernel $\tilde{K}(b;\mu)$ is not calculable. In order to access the contribution in the large b region, the exponential in the second line of Eq. (22) is usually included. Here, the function $g_{j/P}(x,b)$ parametrizes the nonperturbative large b behavior that is intrinsic to the proton target, while g_K parametrizes the nonperturbative large b behavior of the evolution kernel $\tilde{K}(b;\mu)$.

A matching procedure must be introduced with a parameter $b_{\rm max}$ serving as the boundary between the small b and large b regions. The prescription should also allow for a smooth transition from perturbative to nonperturbative regions and avoid the Landau pole singularity in $\alpha_s(\mu)$. There are different choices on the b_* prescription in the literature. A frequently used one is the Collins-Soper-Sterman (CSS) prescription [31]

$$b_* = b/\sqrt{1+b^2/b_{\rm max}^2}, \qquad b_{\rm max} < 1/\Lambda_{\rm QCD}, \tag{23}$$

which guarantees the feature that $b_* \approx b$ at small b value and $b_* \approx b_{\rm max}$ at large b value. To ensure that b_* is always in the perturbative region, the typical value of $b_{\rm max}$ is chosen around 1 GeV^{-1}.

Therefore, the complete result for the Sudakov form factor appearing in Eqs. (20)–(22) can be sketched as follows:

$$S(Q,b) = S_{\rm P}(Q,b_*) + S_{\rm NP}(Q,b), \tag{24}$$

where $S_{\rm P}(Q,b_*)$ and $S_{\rm NP}(Q,b)$ corresponds to the perturbative part and the nonperturbative part of the Sudakov form factor, with the boundary of two parts set by $b_{\rm max}$. The perturbative part $S_{\rm P}(Q,b_*)$ has been studied [39,42,55,56,58] in detail and has the same result for different TMD PDF and FFs,

$$S_{\rm P}(Q,b_*) = \int_{\mu_b^2}^{Q^2}\frac{d\bar{\mu}^2}{\bar{\mu}^2}\left[A(\alpha_s(\bar{\mu}))\ln\frac{Q^2}{\bar{\mu}^2} + B(\alpha_s(\bar{\mu}))\right], \tag{25}$$

where the A and B coefficients in Eq. (25) can be expanded as perturbative series of α_s/π,

$$A = \sum_{n=1}^{\infty} A^{(n)}\left(\frac{\alpha_s}{\pi}\right)^n, \tag{26}$$

$$B = \sum_{n=1}^{\infty} B^{(n)}\left(\frac{\alpha_s}{\pi}\right)^n. \tag{27}$$

In this work, we will take $A^{(n)}$ up to $A^{(2)}$ and $B^{(n)}$ up to $B^{(1)}$ in the accuracy of next-to-leading-logarithmic (NLL) order [31,37,39,53,56,65],

$$A^{(1)} = C_F, \tag{28}$$

$$A^{(2)} = \frac{C_F}{2}\left[C_A\left(\frac{67}{18} - \frac{\pi^2}{6}\right) - \frac{10}{9}T_R n_f\right], \tag{29}$$

$$B^{(1)} = -\frac{3}{2}C_F. \tag{30}$$

In the perturbative region $1/Q \ll b \ll 1/\Lambda$, other important elements are TMD PDFs and FFs at a fixed scale [$\tilde{F}(x,b;\mu)$ and $\tilde{D}(x,b;\mu)$], which can be expressed as the convolution of the perturbatively calculable coefficients C and the corresponding collinear counterparts of TMDs [$F_{i/H}(\xi,\mu)$ and $D_{H/j}(\xi,\mu)$],

$$\tilde{F}(x,b;\mu) = \sum_i \int_x^1 \frac{d\xi}{\xi} C_{q\leftarrow i}(x/\xi,b;\mu) F_{i/H}(\xi,\mu), \tag{31}$$

$$\tilde{D}(z,b;\mu) = \sum_j \int_z^1 \frac{d\xi}{\xi} C_{j\leftarrow q}(z/\xi,b;\mu) D_{H/j}(\xi,\mu). \tag{32}$$

Here, μ is a dynamic scale related to b_* by $\mu = c/b_*$, with $c = 2e^{-\gamma_E}$. The parameter c is chosen to optimize the perturbation expansion such that, in this choice, the order-$\mathcal{O}(\alpha_s)$ result of $K(b_*;\mu)$ vanishes. Note that $C_{q\leftarrow i}(x/\xi,b;\mu) = \sum_{n=0}^{\infty} C_{q\leftarrow i}^{(n)}(\alpha_s/\pi)^n$ and $C_{j\leftarrow q}(z/\xi,b;\mu) = \sum_{n=0}^{\infty} C_{j\leftarrow q}^{(n)}(\alpha_s/\pi)^n$ are the perturbatively calculable coefficient functions.

The nonperturbative part $S_{\rm NP}$ can not be calculated from perturbative QCD. They may be parametrized and extracted from experimental data. There are several different parametrizations on $S_{\rm NP}$ in the literature [31,34,37,40,42,44,51–58]; we will discuss two of them in detail.

A. Approach I

One of the approaches applied in this study is the Echevarria-Idilbi-Kang-Vitev (EIKV parametrization) nonperturbative Sudakov $S_{\rm NP}$ for the unpolarized TMD PDFs and TMD FFs, which has the following form [42]:

$$S_{\rm NP}^{\rm pdf}(b,Q)=b^2\left(g_1^{\rm pdf}+\frac{g_2}{2}\ln\frac{Q}{Q_0}\right), \tag{33}$$

$$S_{\rm NP}^{\rm ff}(b,Q)=b^2\left(g_1^{\rm ff}+\frac{g_2}{2}\ln\frac{Q}{Q_0}\right). \tag{34}$$

Here, g_2 includes the information on the large b behavior of the evolution kernel $\tilde{K}$. ($g_K(b)=g_2b^2$.) This function is universal for different types of TMDs and is spin independent [34,37,42,43]. On the other hand, g_1 contains information on the intrinsic nonperturbative transverse motion of bound partons. It could depend on the type of TMDs and can be interpreted as the intrinsic transverse momentum width for the relevant TMDs at the initial scale Q_0 [37,57,65–67]. Furthermore, $g_1^{\rm pdf}$ and $g_1^{\rm ff}$ are parametrized as follows:

$$g_1^{\rm pdf}=\frac{\langle k_T^2\rangle_{Q_0}}{4}, \tag{35}$$

$$g_1^{\rm ff}=\frac{\langle p_T^2\rangle_{Q_0}}{4z^2}, \tag{36}$$

where $\langle k_T^2\rangle_{Q_0}$ and $\langle p_T^2\rangle_{Q_0}$ are the averaged intrinsic transverse momenta squared for TMD PDFs and FFs at the initial scale Q_0, respectively. In Ref. [42] the authors tuned the current extracted ranges of three parameters $\langle k_T^2\rangle_{Q_0}$, $\langle p_T^2\rangle_{Q_0}$, and g_2 with $Q_0=\sqrt{2.4}$ GeV in Refs. [68–70] and further found that the following values of parameters can reasonably describe the SIDIS data together with the Drell-Yan lepton pair and W/Z boson production data:

$$\langle k_T^2\rangle_{Q_0}=0.38\ \mathrm{GeV}^2,\qquad \langle p_T^2\rangle_{Q_0}=0.19\ \mathrm{GeV}^2,$$
$$g_2=0.16\ \mathrm{GeV}^2,\qquad b_{\rm max}=1.5\ \mathrm{GeV}^{-1}. \tag{37}$$

Since the information of the nonperturbative Sudakov form factor for the polarizing FF of the Λ hyperon still remains unknown, we assume it to be the same as that for the unpolarized TMD FF $S_{\rm NP}^{\rm ff}$.

It is straightforward to rewrite the scale-dependent TMDs $\tilde{F}$ and $\tilde{D}$ in $\boldsymbol{b}_\perp$ space as

$$\tilde{F}_{q/H}(x,b;Q)=e^{-\frac{1}{2}S_{\rm P}(Q,b_*)-S_{\rm NP}^{F_{q/H}}(Q,b)}F_{q/H}(x,\mu), \tag{38}$$

$$\tilde{D}_{H/q}(z,b;Q)=e^{-\frac{1}{2}S_{\rm P}(Q,b_*)-S_{\rm NP}^{D_{H/q}}(Q,b)}D_{H/q}(z,\mu). \tag{39}$$

Hereafter, we apply the leading order (LO) results for the hard coefficients C, $\mathcal{F}$, and $\mathcal{D}$ for f_1, D_1, and $D_{1T}^\perp$, i.e., $C_{q\leftarrow i}^{(0)}=\delta_{iq}\delta(1-x)$, $C_{j\leftarrow q}^{(0)}=\delta_{qj}\delta(1-z)$, $\mathcal{F}(Q)=1$ and $\mathcal{D}(Q)=1$. The factor of $\frac{1}{2}$ in front of $S_{\rm P}$ comes from the fact that $S_{\rm P}$ is equally distributed to the initial-state quark and the final-state quark [71].

With all the above ingredients, we can write down the evolved TMDs explicitly as

$$\tilde{f}_1^{q/p}(x_B,b;Q)=e^{-\frac{1}{2}S_{\rm P}(Q,b_*)-S_{\rm NP}^{\rm pdf}(Q,b)}f_1^{q/p}(x_B,\mu), \tag{40}$$

$$\tilde{D}_1^{\Lambda/q}(z,b;Q)=e^{-\frac{1}{2}S_{\rm P}(Q,b_*)-S_{\rm NP}^{\rm ff}(Q,b)}D_1^{\Lambda/q}(z,\mu), \tag{41}$$

$$\tilde{D}_{1T}^{\perp(\alpha)\Lambda/q}(z,b;Q)=\frac{ib_\perp^\alpha}{2}e^{-\frac{1}{2}S_{\rm P}(Q,b_*)-S_{\rm NP}^{\rm ff}(Q,b)}\hat{D}_{1T}^{\perp(3)}(z,z,\mu). \tag{42}$$

Here, $\hat{D}_{1T}^{\perp(3)}(z,z,\mu)$ is the twist-3 FF of quark flavor q to Λ hyperon, which satisfies the following relation with the polarizing FF $D_{1T}^{\perp\Lambda/q}$ and the first transverse moment of the polarizing FF $D_{1T}^{\perp(1)}$ [72]:

$$\begin{aligned}\hat{D}_{1T}^{\perp(3)}(z,z,\mu)&=\int d^2\boldsymbol{K}_\perp\frac{|\boldsymbol{K}_\perp^2|}{M_\Lambda}D_{1T}^{\perp h/q}(z,\boldsymbol{K}_\perp^2,\mu)\\&=2M_\Lambda D_{1T}^{\perp(1)}(z,\mu).\end{aligned} \tag{43}$$

Thus, the TMDs in the transverse momentum space can be obtained by performing the Fourier transformation,

$$f_1^{q/p}(x_B,p_T;Q)=\int_0^\infty\frac{dbb}{2\pi}J_0(p_Tb)e^{-\frac{1}{2}S_P(Q,b_*)-S_{\rm NP}^{\rm pdf}(Q,b)}f_1^{q/p}(x_B,\mu), \tag{44}$$

$$D_1^{\Lambda/q}(z,K_\perp;Q)=\int_0^\infty\frac{dbb}{2\pi}J_0(K_\perp b/z)e^{-\frac{1}{2}S_P(Q,b_*)-S_{\rm NP}^{\rm ff}(Q,b)}D_1^{\Lambda/q}(z,\mu), \tag{45}$$

$$\frac{K_\perp^\alpha}{M_\Lambda}\tilde{D}_{1T}^{\perp\Lambda/q(\alpha)}(z,K_\perp;Q)=\int_0^\infty\frac{dbb^2}{4\pi}J_1(K_\perp b/z)e^{-\frac{1}{2}S_P(Q,b_*)-S_{\rm NP}^{\rm ff}(Q,b)}D_{1T}^{\perp(3)}(z,z,\mu). \tag{46}$$

where $p_T=|\boldsymbol{p}_T|$, $K_\perp=|\boldsymbol{K}_\perp|$.

B. Approach II

Besides the traditional parametrization [53,54,73] and the EIKV parametrization, some other forms have been also proposed [44,57,64,74] recently. Particularly, a new evolution formalism was proposed by Bacchetta, Delcarro, Pisano, Radici, and Signori (BDPRS parametrization) in Ref. [44] for $\tilde{f}_1^a$ and $\tilde{D}_1^{a\to h}$,

$$\tilde{f}_1^a(x,b^2;Q^2)=f_1^a(x;\mu^2)e^{-S(\mu^2,Q^2)}e^{\frac{1}{2}g_K(b)\ln(Q^2/Q_0^2)}\tilde{f}_{1\rm NP}^a(x,b^2), \tag{47}$$

$$\tilde{D}_1^{a\to h}(z,b^2;Q^2) = D_1^{a\to h}(z;\mu^2)e^{-S(\mu^2,Q^2)}e^{\frac{1}{2}g_K(b)\ln(Q^2/Q_0^2)}\tilde{D}_{1\mathrm{NP}}^{a\to h}(z,b^2), \quad (48)$$

where $g_K = -g_2 b^2/2$, following the choice in Refs. [53,54,73]. Note that $\tilde{f}_{1\mathrm{NP}}^a(x,b^2)$ and $\tilde{D}_{1\mathrm{NP}}^{a\to h}(z,b^2)$ are the intrinsic nonperturbative part of the PDFs and FFs respectively, which are parametrized as

$$\tilde{f}_{1\mathrm{NP}}^a(x,b^2) = \frac{1}{2\pi}e^{-g_1\frac{b^2}{4}}\left(1 - \frac{\lambda g_1^2}{1+\lambda g_1}\frac{b^2}{4}\right), \quad (49)$$

$$\tilde{D}_{1\mathrm{NP}}^{a\to h}(z,b^2) = \frac{g_3 e^{-g_3\frac{b^2}{4z^2}} + (\frac{\lambda_F}{z^2})g_4^2(1-g_4\frac{b^2}{4z^2})e^{-g_4\frac{b^2}{4z^2}}}{2\pi z^2(g_3 + (\frac{\lambda_F}{z^2})g_4^2)}, \quad (50)$$

with

$$g_1(x) = N_1\frac{(1-x)^\alpha x^\sigma}{(1-\hat{x})^\alpha \hat{x}^\sigma}, \quad (51)$$

$$g_{3,4}(z) = N_{3,4}\frac{(z^\beta+\delta)(1-z)^\gamma}{(\hat{z}^\beta+\delta)(1-\hat{z})^\gamma}. \quad (52)$$

Here, $\hat{x} = 0.1$ and $\hat{z} = 0.5$ are fixed, and α, σ, β, γ, δ, $N_1 \equiv g_1(\hat{x})$, $N_{3,4} \equiv g_{3,4}(\hat{z})$ are free parameters fitted to the available data from SIDIS, Drell-Yan, and W/Z boson production processes. Besides the $b_*(b)$ prescription in the original CSS approach [31], there are also several different choices on the form of $b_*(b)$ [44,75]. In Ref. [44], a new b_* prescription different from Eq. (23) was proposed as

$$b_* = b_{\max}\left(\frac{1-e^{-b^4/b_{\max}^4}}{1-e^{-b^4/b_{\min}^4}}\right)^{1/4}. \quad (53)$$

Again, $b_{\max}$ is the boundary of the nonperturbative and perturbative $\boldsymbol{b}_\perp$ space region with fixed value of $b_{\max} = 2e^{-\gamma_E}\ \mathrm{GeV}^{-1} \approx 1.123\ \mathrm{GeV}^{-1}$. Furthermore, the authors in Ref. [44] also chose to saturate b_* at the minimum value $b_{\min} \propto 2e^{-\gamma_E}/Q$.

We note that the above two approaches can reasonably describe the SIDIS, Drell-Yan, and W/Z boson production data, with the values of introduced free parameters. In this work, we will adopt both the EIKV evolution formalism and the BDPRS evolution formalism to estimate the $\sin(\phi_\Lambda - \phi_S)$ asymmetry in SIDIS. The goal is to investigate the impact of the different evolution formalisms on the asymmetry.

IV. NUMERICAL CALCULATION

Using the framework set up above, we perform the numerical calculation on the $\sin(\phi_\Lambda - \phi_S)$ azimuthal asymmetry in the process $e^- p \to e^- \Lambda^\uparrow X$ at the kinematical region of the EIC. To do this we need to know the collinear functions appearing in Eqs. (40)–(42). For the unpolarized PDF $f_1(x,\mu)$ of the proton target, we apply the next-to-leading-order set of the CT10 parametrization (central PDF set) [76]. For the $D_{1T}^{\perp(3)}(z,\mu)$ and $D_1(z,\mu)$ of the Λ hyperon, we adopt two different sets for comparison.

The first set (set I) is the polarizing FF of lambda $D_{1T}^\perp$ for light flavors from the spectator diquark model calculation [29], in which the contributions from both the scalar diquark and the axial-vector diquark spectators are included. Assuming the SU(6) spin-flavor symmetry, the fragmentation functions of the Λ hyperon for light flavors satisfy the relations between different quark flavors and diquark types as

$$D_{1T}^{\perp u} = D_{1T}^{\perp d} = \frac{1}{4}D_{1T}^{\perp(s)} + \frac{3}{4}D_{1T}^{\perp(v)}, \quad D_{1T}^{\perp s} = D_{1T}^{\perp(s)}, \quad (54)$$

where u, d, and s denote the up, down, and strange quarks, respectively. $D_{1T}^{\perp(v)}$ and $D_{1T}^{\perp(s)}$ represent the contribution from the axial-vector diquark and scalar diquark, and their expressions, as well as the values of the parameters, can be found in Refs. [29]. One should notice that in this model only the valence quarks contribute to the Λ fragmentation function, while the sea quark contribution is zero. For consistency, in this set, we apply the FF $D_1^{\Lambda/q}(z)$ from the same model in Ref. [29]. Furthermore, we apply the QCDNUM package [77] to perform the Dokshitzer-Gribov-Lipatov-Altarelli-Parisi evolution of the unpolarized FF $D_1^{\Lambda/q}(z,\mu_b)$ and the polarizing FF $\hat{D}_{1T}^{\perp(3)}(z,z,\mu_b)$ from the model scale Q_0 to another energy since the evolution kernel for the diagonal piece of $\hat{D}_{1T}^{\perp(3)}(z,z,\mu_b)$ is the same as that for the unpolarized FF [78].

The second set (set II) of the FFs is the parametrization of the Λ polarizing FF in Ref. [26], extracted from the Belle experimental data on the $\Lambda/\bar{\Lambda}$ polarization in the e^+e^- annihilation process, in which the inclusive (plus a jet) Λ and associated production of a light charged hadron is measured. In Ref. [26], the first transverse-moment of $D_{1T}^\perp$ is given by

$$D_{1T}^{\perp(1)}(z) = \sqrt{\frac{e}{2}}\frac{1}{zM_\Lambda}\frac{1}{M_{\mathrm{pol}}}\frac{\langle K_\perp^2\rangle_{\mathrm{pol}}^2}{\langle K_\perp^2\rangle}\Delta D_{\Lambda^\uparrow/q}(z), \quad (55)$$

with

$$\langle K_\perp^2\rangle_{\mathrm{pol}} = \frac{M_{\mathrm{pol}}^2}{M_{\mathrm{pol}}^2 + \langle K_\perp^2\rangle}\langle K_\perp^2\rangle, \quad (56)$$

where the unpolarized Gaussian width $\langle K_\perp^2\rangle = 0.2\ \mathrm{GeV}^2$ [68] and the z-dependent part of the polarizing FF $\Delta D_{\Lambda^\uparrow/q}(z)$ was parameterized as

$$\Delta D_{\Lambda^\uparrow/q}(z) = N_q z^{a_q}(1-z)^{b_q}\frac{(a_q+b_q)^{a_q+b_q}}{a_q{}^{a_q}b_q{}^{b_q}}D_{\Lambda/q}(z). \quad (57)$$

Here, the Albino-Kniehl-Kramer 08 [79] set for unpolarized Λ FF $D_{\Lambda/q}(z)$ is adopted. Since the Λ FF sets are given for $\Lambda+\bar{\Lambda}$, the two contributions are separated as [26]

$$D_{\bar{\Lambda}/q}(z_p) = D_{\Lambda/\bar{q}}(z_p) = (1-z_p)D_{\Lambda/q}(z_p), \quad (58)$$

where the scaling variable z_p is related to z by $z_p \simeq z[1-M_\Lambda^2/(z^2Q^2)]$. The corresponding collinear twist-3 fragmentation function of quark flavor q to Λ hyperon $\hat{D}_{1T}^{\perp(3)}(z,z,\mu_b)$ can also be obtained by using Eq. (43). The best fit of the parameters in Eq. (57) are obtained as

$$\begin{aligned}
&N_u = 0.47^{+0.32}_{-0.20}, \qquad N_d = -0.32 \pm 0,13,\\
&N_s = -0.57^{+0.29}_{-0.43}, \qquad a_u = 0, \qquad a_d = 0,\\
&a_s = 2.30^{1.08}_{-0.91}, \qquad b_u = 3.50^{+2.33}_{-1.82}, \qquad b_d = 0,\\
&b_s = 0, \qquad \langle K_\perp^2\rangle_{\mathrm{pol}} = 0.1 \pm 0.02\ \mathrm{GeV}^2. \qquad (59)
\end{aligned}$$

We apply the kinematical ranges of the EIC as follows [80]:

$$\begin{aligned}
&0.001 < x < 0.4, \qquad 0.07 < y < 0.9, \qquad 0.2 < z < 0.75,\\
&1\ \mathrm{GeV}^2 < Q^2, \qquad W > 5\ \mathrm{GeV},\\
&\sqrt{s} = 45\ \mathrm{GeV}, \qquad P_{\Lambda T} < 0.5\ \mathrm{GeV}, \qquad (60)
\end{aligned}$$

with $W^2 = (P+q)^2 \approx \frac{1-x}{x}Q^2$ being the invariant mass of the virtual photon-nucleon system. Using the above kinematical configurations and applying Eqs. (4), (9), and (11), we numerically estimate the $\sin(\phi_\Lambda - \phi_S)$ asymmetry in the electroproduction of transversely polarized Λ at the EIC. The corresponding numerical results are plotted in Figs. 1 and 2, in which the left, middle, and right panels show the $\sin(\phi_\Lambda - \phi_S)$ azimuthal asymmetry as functions of $P_{\Lambda T}$, x, and z, respectively. In order to estimate, the predicted asymmetry are also plotted as red points with the statistical error bars in the figures. The statistical errors δA are obtained from the unpolarized cross section σ and the integrated luminosity $\mathcal{L}$ through the relation [81]

$$\delta A = \frac{1}{\sqrt{\mathcal{L}\sigma}}. \quad (61)$$

In this work, the integrated luminosity is adopted as $\mathcal{L} = 100\ \mathrm{fb}^{-1}$ for the EIC [82]. Since the statistical errors are too small to be depicted, the error bars in the figures are enlarged by a factor 10. It can be found that the statistical errors are quite small, which will make the measurement possible, however, we should note that there are no systematic errors being estimated in the figures.

Figure 1 plots the asymmetries calculated from the spectator diquark model result (set I) of the Λ polarizing FF [29]. Here, two different approaches for the nonperturbative Sudakov form factor in the TMD evolution formalism are adopted for comparison. The dashed lines correspond to the asymmetry from the EIKV parametrization [42] (approach I) on S_{NP} combined with the b_* prescription in Eq. (23). The shaded areas show the uncertainty bands due to the uncertainties of the parameters. The solid lines show the asymmetry calculated from the BDPRS parametrization (approach II) [44] on the nonperturbative Sudakov form factor. In this calculation, the b_* prescription in Eq. (53) is used, which is different from the CSS prescription. As depicted in Fig. 1, in all cases the $\sin(\phi_\Lambda - \phi_S)$ azimuthal asymmetries are negative and sizable. The minus sign of the asymmetry comes from the negative results of Λ polarizing FFs in our model calculation. In addition, the magnitude of asymmetry decreases with increasing x, while it increases with increasing $P_{\Lambda T}$ or z. Moreover, we find that different approaches

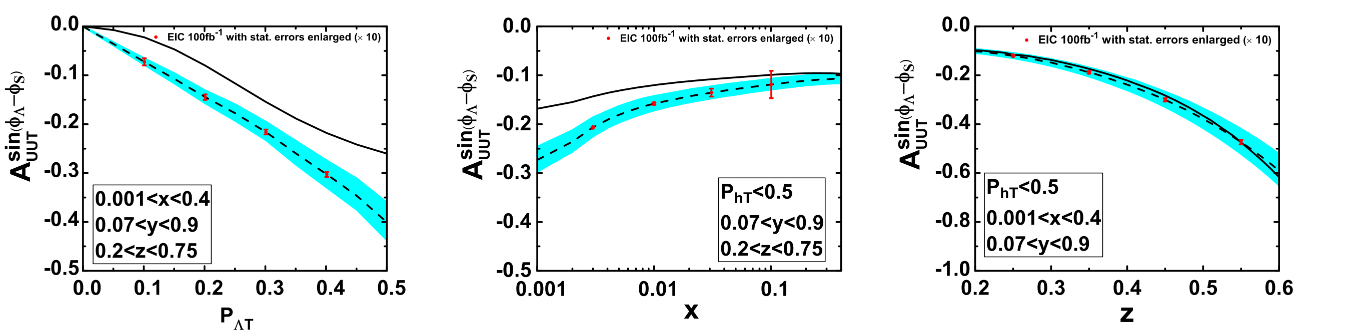

FIG. 1. The $\sin(\phi_\Lambda - \phi_S)$ azimuthal asymmetry in SIDIS process $lp \to \Lambda^\uparrow + X$. The solid lines correspond to the results from the BDPRS parametrization [44] [Eqs. (47) and (48)] on the nonperturbative form factor, while the dashed lines correspond to the results calculated from the EIKV parametrization [42] [Eqs. (33) and (34)]. The shaded areas show the uncertainty bands determined by the uncertainties of the parameters. In this calculation the spectator model result for the Λ polarizing FF is adopted. The statistical errors from experimental measurements at the EIC ($\mathcal{L} = 100\ \mathrm{fb}^{-1}$) are depicted with red bars for several points. Since the statistical error bars are too small, they are enlarged by a factor of 10 to make them visible.

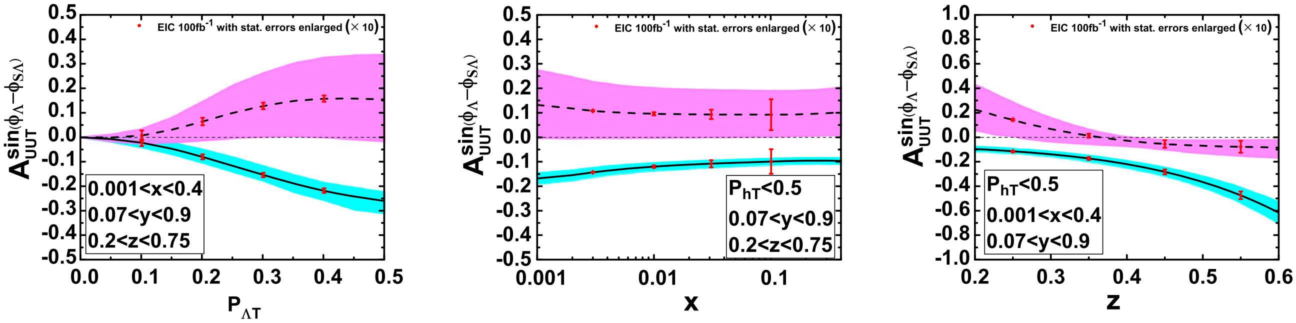

FIG. 2. Comparison between the asymmetry from the set I result (spectator model result [29]) and that from the set II result (parametrization in [26]) for the Λ polarizing FF, depicted by the solid lines and dashed lines, respectively. The shaded areas show the uncertainty bands determined by the uncertainties of the parameters. In this calculation the BDPRS parametrization [44] for the TMD evolution is adopted. The statistical errors from experimental measurements at the EIC ($\mathcal{L} = 100\ \mathrm{fb}^{-1}$) are depicted with red bars for several points. Since the statistical error bars are very small, they are enlarged by a factor of 10 to make them visible.

dealing with the nonperturbative part of evolution lead to the same signs and the tendencies of the asymmetries, although the size of x-dependent and $P_{\Lambda T}$-dependent asymmetries are somewhat different. For the z-dependent asymmetry, it is found that the two approaches lead to very similar results.

To investigate the dependence of the asymmetry on different choices of the Λ polarizing FFs, we also adopt the parametrization in (55) [26] to calculate the $\sin(\phi_\Lambda - \phi_S)$ asymmetry in SIDIS. The results are plotted by the dashed lines in Fig. 2. The solid lines denote the results (solid lines in Fig. 1) from the spectator model calculation for the Λ polarizing FF for comparison. In this calculation, we utilize the BDPRS parametrization (approach II) on the nonperturbative part of the TMD evolution formalism. Again, the shaded areas in Fig. 2 show the uncertainty bands determined by the uncertainties of the parameters in the extraction of the polarizing FF. We find that the magnitude of the $P_{\Lambda T}$- and x-dependent asymmetries calculated from the parametrization for Λ polarizing FF in Ref. [26] is similar to the results using the Λ polarizing FF from the spectator model, however, the sign of the asymmetry is opposite to that from the spectator model result. Furthermore, the results calculated from the parametrization shows a node in the z-dependent asymmetry. This is because the extracted Λ polarizing FF for the up quark in Ref. [26] is positive, while that for the down quark is negative. Thus, future experimental data on the $\sin(\phi_\Lambda - \phi_S)$ asymmetry of Λ production in SIDIS with high precision at the EIC can discriminate different results for the Λ polarizing FF. We also note there is a relatively large uncertainty band since in this calculation the errors of the parameters of the Λ polarizing FF have also been included.

Finally, we would like to comment on the uncertainties and assumptions applied in the calculations, which lead to the uncertainties of the asymmetry. From the theoretical point of view, there are several sources which will contribute to the uncertainties of the predicted asymmetry in Figs. 1 and 2, as listed in the following:

(1) The uncertainties from the collinear PDF $f_1(x,\mu)$ and the collinear polarizing fragmentation function (PFF) $D_{1T}^{\perp(3)}(z,\mu)$ of the Λ hyperon. As $f_1(x,\mu)$ appears in both the numerator and the denominator, and we calculate the ratio, the uncertainty from $f_1(x,\mu)$ to the asymmetry almost cancels. In the case of the spectator model result (set I) for the FFs, the parameters in the model calculation are fixed and uncertainties are not provided in Ref. [29], therefore, in the asymmetry predicted from set I FFs, the uncertainties from the PFF is not included. In the case of the parametrization for the FFs (set II), the errors for the parameters are given in Ref. [26]. Thus, in this case we include the uncertainties from the FFs of set II in the calculation.

(2) The uncertainty from the nonperturbative evolution of TMDs, i.e., the nonperturbative Sudakov form factors. In the case of EIKV parametrization, the errors for the parameters g_1 and g_2 are also unknown. Furthermore, in both the EIKV and BDPRS parametrizations we assume a universal intrinsic transverse momentum dependence for the fragmented hadron (g_1^{ff} in EIKV parametrization and $D_{1\mathrm{NP}}$ in BDPRS parametrization), as there is no information for the Λ hyperon. Therefore, in calculation of the asymmetry from EIKV parametrization, the uncertainties on the parameters for the nonperturbative Sudakov form factors are not considered.

(3) The uncertainty from the order of perturbative calculations, which include the hard coefficient $C_{q\leftarrow i}$ and the perturbative Sudakov form factor S_P. In our calculation we apply the LO results for $C_{q\leftarrow i}$ and the NLL result for S_P. We note that higher order corrections to $C_{q\leftarrow i}$ and S_P may also bring uncertainties to the asymmetry.

Therefore, the uncertainty bands shown in Figs. 1 and 2 only represent the errors from the known nominal errors on the extracted parameters, and they (particularly the band in

Fig. 1 and the one around the solid line in Fig. 2) should be much larger if all the uncertainties mentioned above are considered. However, we expect these uncertainties will not change the sign of the asymmetries. Further studies are needed in order to provide more precise phenological analysis on the $\sin(\phi_\Lambda - \phi_S)$ asymmetry of electroproduction of the Λ hyperon.

V. CONCLUSION

In this work, we have applied the TMD factorization approach to study the $\sin(\phi_\Lambda - \phi_S)$ azimuthal asymmetry in the $e^- p \to e^- \Lambda^\uparrow X$ process at the kinematical region of the EIC. The asymmetry arises from the convolution of the polarizing FF $D_{1T}^\perp$ for Λ hyperon and the unpolarized PDF f_1 for the proton. We have taken into account the TMD evolution effects of the unpolarized FF and the transversely polarizing FF $D_{1T}^\perp$ of Λ hyperon. In practical calculation we have taken into account two approaches for the TMD evolution for comparison. One is the EIKV approach, the other is the BDPRS approach. Their main difference is the treatment on the nonperturbative part of evolution, while the perturbative part in the two approaches is the same and has been kept at NLL accuracy in this work. As the nonperturbative Sudakov form factor associated with the Λ polarizing FF is still unknown, we assume that it has the same form as that of the unpolarized fragmentation function. The hard coefficients associated with the corresponding collinear functions in the TMD evolution formalism are kept at leading-order accuracy. For the Λ polarizing FF at fixed scale, the model result from the diquark spectator model and the extraction from the Belle e^+e^- data have been adopted to estimate the asymmetry.

The numerical calculations show that different choices of nonperturbative Sudakov form factors in the TMD evolution formalism lead to similar results for $\sin(\phi_\Lambda - \phi_S)$ asymmetry at the energy scale of the EIC, particularly in the z-dependent asymmetry. The asymmetry utilizing the spectator model for the Λ polarizing FF is negative in the entire kinematical region since the polarizing FFs of Λ for u and d quarks are both negative, due to the assumption of $SU(6)$ spin-flavor symmetry. As a comparison, the x-dependent and $P_{\Lambda T}$-dependent asymmetries calculated from the parametrization for the Λ polarizing FF show positive values, and there is a node in the z-dependent asymmetry. Our study demonstrates that a different choice on the Λ polarizing FF can lead to a very different asymmetry in SIDIS. We have also provided detailed discussion on the assumptions and approximations applied in the calculation, which can lead to large uncertainties of the asymmetry. However, we expect these uncertainties will not change the sign of the asymmetries. As a contrast, the projected statistical errors are rather small at the EIC with high luminosity, which will make the future measurement on the asymmetry possible. Thus, future experimental data on the $\sin(\phi_\Lambda - \phi_S)$ asymmetry of Λ production in SIDIS with high precision at the EIC can discriminate different results for the Λ polarizing FF.

ACKNOWLEDGMENTS

This work is partially supported by the NSFC (China) Grants No. 11575043, No. 11905187, and No. 11847217. X. W. is supported by the China Postdoctoral Science Foundation under Grant No. 2018M640680 and the Academic Improvement Project of Zhengzhou University.

[1] A. Lesnik, D. M. Schwartz, I. Ambats, E. Hayes, W. T. Meyer, C. E. W. Ward, T. M. Knasel, E. G. Swallow, R. Winston, and T. A. Romanowski, Phys. Rev. Lett. **35**, 770 (1975).
[2] G. Bunce *et al.*, Phys. Rev. Lett. **36**, 1113 (1976).
[3] G. L. Kane, J. Pumplin, and W. Repko, Phys. Rev. Lett. **41**, 1689 (1978).
[4] W. G. D. Dharmaratna and G. R. Goldstein, Phys. Rev. D **53**, 1073 (1996).
[5] B. Q. Ma, I. Schmidt, J. Soffer, and J. J. Yang, Phys. Rev. D **64**, 014017 (2001); **64**, 099901(E) (2001).
[6] R. L. Jaffe, Phys. Rev. D **54**, R6581 (1996).
[7] M. Burkardt and R. L. Jaffe, Phys. Rev. Lett. **70**, 2537 (1993).
[8] K. Kanazawa, A. Metz, D. Pitonyak, and M. Schlegel, Phys. Lett. B **744**, 385 (2015).
[9] D. Boer, Z. B. Kang, W. Vogelsang, and F. Yuan, Phys. Rev. Lett. **105**, 202001 (2010).
[10] M. Anselmino, D. Boer, U. D'Alesio, and F. Murgia, Phys. Rev. D **65**, 114014 (2002).
[11] M. Anselmino, D. Boer, U. D'Alesio, and F. Murgia, Phys. Rev. D **63**, 054029 (2001).
[12] P. J. Mulders and R. D. Tangerman, Nucl. Phys. **B461**, 197 (1996); **B484**, 538(E) (1997).
[13] D. W. Sivers, Phys. Rev. D **41**, 83 (1990).
[14] D. W. Sivers, Phys. Rev. D **43**, 261 (1991).
[15] D. Boer, arXiv:0907.1610.
[16] K. Ackerstaff *et al.* (OPAL Collaboration), Eur. Phys. J. C **2**, 49 (1998).
[17] D. Boer, R. Jakob, and P. J. Mulders, Nucl. Phys. **B504**, 345 (1997).
[18] S. Y. Wei, K. b. Chen, Y. k. Song, and Z. t. Liang, Phys. Rev. D **91**, 034015 (2015).
[19] Y. Guan *et al.* (Belle Collaboration), Phys. Rev. Lett. **122**, 042001 (2019).

[20] K. J. Heller *et al.*, Phys. Rev. Lett. **41**, 607 (1978); **45**, 1043(E) (1980).
[21] D. de Florian, M. Stratmann, and W. Vogelsang, Phys. Rev. D **57**, 5811 (1998).
[22] A. Airapetian *et al.* (HERMES Collaboration), Phys. Rev. Lett. **94**, 012002 (2005).
[23] Y. Koike, A. Metz, D. Pitonyak, K. Yabe, and S. Yoshida, Phys. Rev. D **95**, 114013 (2017).
[24] L. Gamberg, Z. B. Kang, D. Pitonyak, M. Schlegel, and S. Yoshida, J. High Energy Phys. 01 (2019) 111.
[25] M. Anselmino, R. Kishore, and A. Mukherjee, Phys. Rev. D **100**, 014029 (2019).
[26] U. D'Alesio, F. Murgia, and M. Zaccheddu, Phys. Rev. D **102**, 054001 (2020).
[27] D. Callos, Z. B. Kang, and J. Terry, Phys. Rev. D **102**, 096007 (2020).
[28] K. B. Chen, Z. T. Liang, Y. L. Pan, Y. K. Song, and S. Y. Wei, Phys. Lett. B **816**, 136217 (2021).
[29] Y. Yang, Z. Lu, and I. Schmidt, Phys. Rev. D **96**, 034010 (2017).
[30] J. C. Collins and D. E. Soper, Nucl. Phys. **B193**, 381 (1981); **B213**, 545(E) (1983).
[31] J. C. Collins, D. E. Soper, and G. F. Sterman, Nucl. Phys. **B250**, 199 (1985).
[32] X. D. Ji, J. P. Ma, and F. Yuan, Phys. Rev. D **71**, 034005 (2005).
[33] X. d. Ji, J. P. Ma, and F. Yuan, Phys. Lett. B **597**, 299 (2004).
[34] J. Collins, Camb. Monogr. Part. Phys. Nucl. Phys. Cosmol. **32** (2011), http://www.cambridge.org/de/knowledge/isbn/item5756723.
[35] D. Boer, Nucl. Phys. **B806**, 23 (2009).
[36] S. Arnold, A. Metz, and M. Schlegel, Phys. Rev. D **79**, 034005 (2009).
[37] S. M. Aybat and T. C. Rogers, Phys. Rev. D **83**, 114042 (2011).
[38] J. C. Collins and T. C. Rogers, Phys. Rev. D **87**, 034018 (2013).
[39] M. G. Echevarria, A. Idilbi, A. Schäfer, and I. Scimemi, Eur. Phys. J. C **73**, 2636 (2013).
[40] M. G. Echevarra, A. Idilbi, and I. Scimemi, Phys. Lett. B **726**, 795 (2013).
[41] D. Pitonyak, M. Schlegel, and A. Metz, Phys. Rev. D **89**, 054032 (2014).
[42] M. G. Echevarria, A. Idilbi, Z. B. Kang, and I. Vitev, Phys. Rev. D **89**, 074013 (2014).
[43] Z. B. Kang, A. Prokudin, P. Sun, and F. Yuan, Phys. Rev. D **93**, 014009 (2016).
[44] A. Bacchetta, F. Delcarro, C. Pisano, M. Radici, and A. Signori, J. High Energy Phys. 06 (2017) 081; 06 (2019) 051(E).
[45] X. Wang, Z. Lu, and I. Schmidt, J. High Energy Phys. 08 (2017) 137.
[46] X. Wang and Z. Lu, Phys. Rev. D **97**, 054005 (2018).
[47] H. Li, X. Wang, and Z. Lu, Phys. Rev. D **101**, 054013 (2020).
[48] A. Idilbi, X. d. Ji, J. P. Ma, and F. Yuan, Phys. Rev. D **70**, 074021 (2004).
[49] J. C. Collins and F. Hautmann, Phys. Lett. B **472**, 129 (2000).
[50] H. Li, X. Wang, Y. Yang, and Z. Lu, Eur. Phys. J. C **81**, 289 (2021).
[51] C. T. H. Davies, B. R. Webber, and W. J. Stirling, Nucl. Phys. **B256**, 413 (1985).
[52] R. K. Ellis, D. A. Ross, and S. Veseli, Nucl. Phys. **B503**, 309 (1997).
[53] F. Landry, R. Brock, P. M. Nadolsky, and C. P. Yuan, Phys. Rev. D **67**, 073016 (2003).
[54] A. V. Konychev and P. M. Nadolsky, Phys. Lett. B **633**, 710 (2006).
[55] S. M. Aybat, J. C. Collins, J. W. Qiu, and T. C. Rogers, Phys. Rev. D **85**, 034043 (2012).
[56] Z. B. Kang, B. W. Xiao, and F. Yuan, Phys. Rev. Lett. **107**, 152002 (2011).
[57] P. Sun, J. Isaacson, C.-P. Yuan, and F. Yuan, Int. J. Mod. Phys. A **33**, 1841006 (2018).
[58] M. G. Echevarria, A. Idilbi, and I. Scimemi, Phys. Rev. D **90**, 014003 (2014).
[59] V. Barone, A. Drago, and P. G. Ratcliffe, Phys. Rep. **359**, 1 (2002).
[60] V. Barone, F. Bradamante, and A. Martin, Prog. Part. Nucl. Phys. **65**, 267 (2010).
[61] Y. Yang and Z. Lu, Phys. Rev. D **95**, 074026 (2017).
[62] D. Boer *et al.*, arXiv:1108.1713.
[63] D. Boer, Phys. Rev. D **60**, 014012 (1999).
[64] J. Collins and T. Rogers, Phys. Rev. D **91**, 074020 (2015).
[65] J. w. Qiu and X. f. Zhang, Phys. Rev. Lett. **86**, 2724 (2001).
[66] J. w. Qiu and X. f. Zhang, Phys. Rev. D **63**, 114011 (2001).
[67] M. Anselmino, M. Boglione, and S. Melis, Phys. Rev. D **86**, 014028 (2012).
[68] M. Anselmino, M. Boglione, U. D'Alesio, A. Kotzinian, F. Murgia, and A. Prokudin, Phys. Rev. D **71**, 074006 (2005).
[69] J. C. Collins, A. V. Efremov, K. Goeke, S. Menzel, A. Metz, and P. Schweitzer, Phys. Rev. D **73**, 014021 (2006).
[70] P. Schweitzer, T. Teckentrup, and A. Metz, Phys. Rev. D **81**, 094019 (2010).
[71] A. Prokudin, P. Sun, and F. Yuan, Phys. Lett. B **750**, 533 (2015).
[72] F. Yuan and J. Zhou, Phys. Rev. Lett. **103**, 052001 (2009).
[73] P. M. Nadolsky, D. R. Stump, and C. P. Yuan, Phys. Rev. D **61**, 014003 (1999); **64**, 059903(E) (2001).
[74] C. A. Aidala, B. Field, L. P. Gamberg, and T. C. Rogers, Phys. Rev. D **89**, 094002 (2014).
[75] J. Collins, L. Gamberg, A. Prokudin, T. C. Rogers, N. Sato, and B. Wang, Phys. Rev. D **94**, 034014 (2016).
[76] H. L. Lai, M. Guzzi, J. Huston, Z. Li, P. M. Nadolsky, J. Pumplin, and C.-P. Yuan, Phys. Rev. D **82**, 074024 (2010).
[77] M. Botje, Comput. Phys. Commun. **182**, 490 (2011).
[78] Z. B. Kang, Phys. Rev. D **83**, 036006 (2011).
[79] S. Albino, B. A. Kniehl, and G. Kramer, Nucl. Phys. **B803**, 42 (2008).
[80] A. Accardi *et al.*, Eur. Phys. J. A **52**, 268 (2016).
[81] X. Chu, E. C. Aschenauer, J. H. Lee, and L. Zheng, Phys. Rev. D **96**, 074035 (2017).
[82] R. Abdul Khalek, A. Accardi, J. Adam, D. Adamiak, W. Akers, M. Albaladejo, A. Al-bataineh, M. G. Alexeev, F. Ameli, P. Antonioli *et al.*, arXiv:2103.05419.